Magnetic properties of Sn-substituted Ni–Zn ferrites synthesized from nano-sized powders of NiO, ZnO, Fe_2O_3, and SnO_2

M A Ali[1], M M Uddin[1,†], M N I Khan[2], F U Z Chowdhury[1], S M Hoque[2], and S I Liba[2]

[1] *Department of Physics, Chittagong University of Engineering and Technology (CUET), Chittagong* 4349, *Bangladesh*
[2] *Materials Science Division, Atomic Energy Center, Dhaka* 1000, *Bangladesh*

(Received 14 February 2017; revised manuscript received 12 March 2017; published online 17 May 2017)

A series of $Ni_{0.6-x/2}Zn_{0.4-x/2}Sn_xFe_2O_4$ ($x = 0.0$, 0.05, 0.1, 0.15, 0.2, and 0.3) (NZSFO) ferrite composities have been synthesized from nano powders using a standard solid state reaction technique. The spinel cubic structure of the investigated samples has been confirmed by x-ray diffraction (XRD). The magnetic properties such as saturation magnetization (M_s), remanent magnetization (M_r), coercive field (H_c), and Bohr magneton (μ) are calculated from the hysteresis loops. The value of M_s is found to decrease with increasing Sn content in the samples. This change is successfully explained by the variation of *A*–*B* interaction strength due to Sn substitution in different sites. The compositional stability and quality of the prepared ferrite composites have also been endorsed by the fairly constant initial permeability (μ') over a wide range of frequency. The decreasing trend of μ' with increasing Sn content has been observed. Curie temperature T_C has been found to increase with the increase in Sn content. A wide spread frequency utility zone indicates that the NZSFO can be considered as a good candidate for use in broadband pulse transformers and wide band read-write heads for video recording. The composition of $x = 0.05$ shows unusual results and the possible reason is also mentioned with the established formalism.

Keywords: magnetic properties, saturation magnetization, permeability, Curie temperature

PACS: 75.50.Bb, 75.50.Gg, 75.60.Ej, 75.50.Ss **DOI:** 10.1088/1674-1056/26/7/077501

1. Introduction

Over the last few decades, the scientific community has paid significant attention to the spinel ferrites due to their fascinating properties that meet the requirements of various applications. No other magnetic materials can replace the ferrites due to their low price, availability, and stability. The Ni–Zn ferrites have become an important candidate in high frequency applications due to their high electrical resistivity, high permeability, compositional stability, and low eddy current losses.[1–6] The uniqueness of the Ni–Zn ferrites is motivating numerous researchers to open the way for commercial applications and new types of ferrites are unveiled with excellent properties for practical application. The properties of the Ni–Zn ferrites can be tailored by altering the chemical composition, preparation methods, sintering temperature (T_s), and impurity element or levels.[5–28] Recently, many researchers reported the structural, magnetic, and electrical properties of Ni–Zn ferrites and/or substituted Ni–Zn ferrites in bulk[6,12,13,19–21,26–28] and nano forms.[16,22–24]

The properties of the Ni–Zn ferrites can be changed remarkably by substitution of tetravalent ions such as Ti^{4+} and Sn^{4+}. Investigations on the substitution of Sn^{4+} have been reported by many researchers.[6,9–11] We reported the structural, morphological, and electrical properties of Sn-substituted Ni–Zn ferrites.[6] Das *et al*. reported the variation of the lattice parameter, saturation magnetization, and Curie temperature with Ti^{4+}, Zr^{4+}, and Sn^{4+} substitution in Ni–Zn ferrites synthesized by the chemical method.[9] The Sn^{4+} substituted $Ni_{1-y}Zn_yFe_2O_4$ ($y = 0.3$, 0.4) ferrite samples were prepared in an oxidizing atmosphere using the solution technique and the Mössbauer and magnetization properties were investigated by Khan *et al*.[10] The magnetic hysteresis and the thermal variation of the magnetic parameters in the Sn^{4+} doped Ni–Zn ferrites prepared by the standard ceramic technique were reported by Maskar *et al*.[11] We have synthesized the Sn^{4+} substituted Ni–Zn ferrites using nano powders (which is different from the work by Maskar *et al.*[11]) by the standard ceramic technique. Another significant dissimilarity is that they have doped Sn in the Ni–Zn ferrites, while we have simultaneously substituted Sn for both Ni and Zn. The characterization and frequency dependence of the magnetic properties of the Ni–Sn–Zn ferrites provide a way to classify the ferrites for particular applications. The information would be very useful for the scientific community in this regard.

To the best of our knowledge, the study of Ni–Zn ferrites prepared from nano powders has not been reported yet. Here, we report the magnetic properties of Sn-substituted $Ni_{0.6}Zn_{0.4}Fe_2O_4$ ferrites prepared from nano-sized raw materials by the solid state reaction technique.

†Corresponding author. E-mail: mohi@cuet.ac.bd

© 2017 Chinese Physical Society and IOP Publishing Ltd

2. Materials and methods

A solid state reaction route was followed to synthesize Sn substituted Ni–Zn ferrite $Ni_{0.6-x/2}Zn_{0.4-x/2}Sn_xFe_2O_4$ ($0.0 \leq x \leq 0.30$) (NZSFO). High purity (99.5%) (US Research Nanomaterials, Inc.) oxides of nano powders were used as the raw materials. The particle size of nickel oxide (NiO), zinc oxide (ZnO), iron oxide (Fe_2O_3), and tin oxide (SnO_2) are 20–40 nm, 15–35 nm, 35–45 nm, and 35–55 nm, respectively. The detail of the preparation technique has been described elsewhere.[5,6] The phase formation and surface morphology of the synthesized samples were studied by x-ray diffraction (XRD) using a Philips X'pert PRO x-ray diffractometer (PW3040) with Cu K_α radiation ($\lambda = 1.5405$ Å) and scanning electron microscope (SEM), respectively. The magnetic properties (M–H curve, saturation magnetization M_s, coercive field H_c, and Bohr magneton) were elucidated by a vibrating sample magnetometer (VSM) (Micro Sense EV9) with a maximum applied field of 10 kOe. Frequency and temperature dependent permeability was investigated by using a Wayne Kerr precision impedance analyzer (6500B). An applied voltage of 0.5 V with a low inductive coil was used to measure the permeability.

3. Results and discussion

3.1. XRD analysis

The XRD patterns of the Sn-substituted Ni–Zn ferrites $Ni_{0.6-x/2}Zn_{0.4-x/2}Sn_xFe_2O_4$ are shown in Fig. 1. The XRD spectra are indexed and an fcc cubic phase is identified. The structural parameters are calculated from the XRD data and have been discussed by Ali *et al.*[6] The lattice constants are calculated from the XRD data and listed in Table 1.

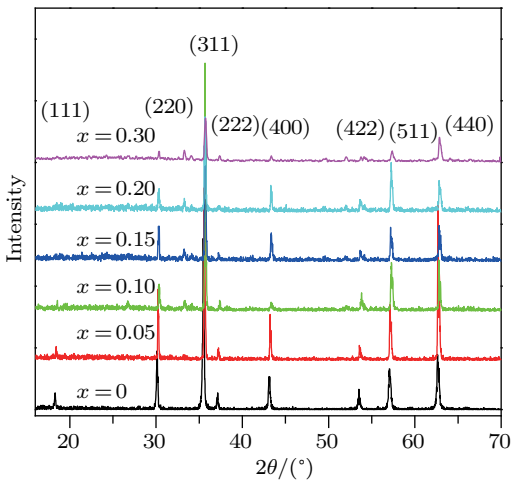


Fig. 1. (color online) XRD patterns of $Ni_{0.6-x/2}Zn_{0.4-x/2}Sn_xFe_2O_4$ ($x = 0.0$, 0.05, 0.1, 0.15, 0.2 0.3, and 0.4).[6]

The distances between the magnetic ions at tetrahedral (A) and octahedral (B) sites are calculated using the equations $L_A = a\frac{\sqrt{3}}{4}$ and $L_B = a\frac{\sqrt{3}}{2}$. The values are also listed in Table 1. The hopping lengths L_A and L_B decrease with increasing Sn concentration, this might be because the lattice parameters of the Ni–Zn ferrites decrease with increasing Sn^{4+} concentration.

3.2. Magnetic properties

The plots of applied magnetic field H (up to 10 kOe) dependent magnetization at room temperature of $Ni_{0.6-x/2}Zn_{0.4-x/2}Sn_xFe_2O_4$ ($x = 0.0$, 0.05, 0.1, 0.15, 0.2, and 0.3) ceramics sintered at 1300 °C are shown in Fig. 2.

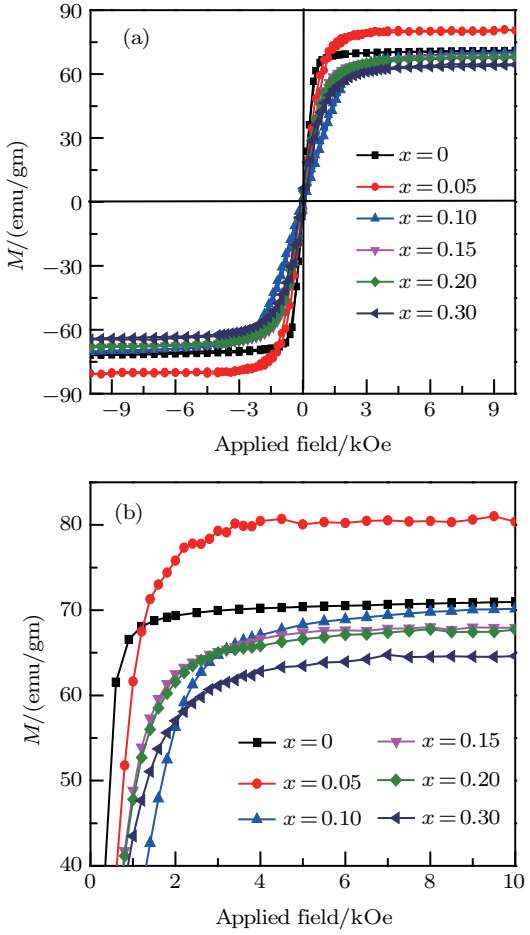


Fig. 2. (color online) (a) The M–H loops of the NZSFO ferrite samples, (b) magnification of the upper saturated part of the M–H loops.

The magnetization increases with increasing the applied magnetic field up to a certain field above which the sample becomes saturated. The saturation magnetization M_s, coercive field H_c, remanent magnetization M_r, and Bohr magneton μ are also calculated from the measured magnetic hysteresis loop and presented in Table 1. It is seen that the H_c of the Sn-substituted samples (NZSFO) are larger than that of the parent (NZFO) and it could be inferred that the prepared ferrites are not reasonably soft in nature.

The variation of saturation magnetization M_s with Sn content of the NZSFO is shown in Table 1. The value of M_s shows

a decreasing trend with increasing x except $x = 0.05$ where the M_s increases slightly. This characteristic can be understood in terms of exchange interactions of cations in the samples. However, the AB interactions are generally dominant in the ferrites, the AA and BB interactions can no longer be ignored. The magnetic moment of the Ni ion is affected by the modified strength of the $Ni^{2+} \leftrightarrow O^{2-} \leftrightarrow Ni^{2+}$ interactions due to the presence of non-magnetic ions Sn and Zn in the samples.

Table 1. The lattice constant a_{expt}, average grain size D_g, magnetic cation hopping lengths L_A and L_B, saturation magnetization M_s, coercive field H_c, remanent magnetization M_r, and Bohr magneton μ of NZSFO for different x.

x	a_{expt}/Å	D_g/μm	L_A/Å	L_B/Å	M_s/(emu/gm)	H_c/Oe	M_r/(emu/gm)	μ/μ_B
0.00	8.39311	07.8	3.6343	7.2686	72.73 60.0[9] 96.0 [11]	1.26	0.16	3.09
0.05	8.38996	10.1	3.6329	7.2659	80.82	67.25	5.00	3.48
0.10	8.37546	18.8	3.6266	7.2533	70.23	62.41	2.07	3.07
0.15	8.38137	21.0	3.6292	7.2584	68.09	71.82	4.55	3.02
0.20	8.37665	30.1	3.6271	7.2543	68.07	78.10	5.16	3.06
0.30	8.34531	34.8	3.6136	7.2272	64.47	94.47	6.40	2.99

It is assumed that the Sn ions occupy tetrahedral (A) sites initially at lower Sn concentrations however, they reside in B sites at higher Sn concentrations, leading to the reduction of A–A interactions. Consequently, the net magnetic moment, $\bar{M} = \bar{M}_B - \bar{M}_A$, increases in the samples. On further increase of the substituting Sn ions, they enter into B-sites and push some Fe^{3+} ions into A-sites, resulting in the decrease of the magnetic ion density in the B sub-lattice. The concentration of Fe^{3+} ions decreases in the B sub-lattice while it increases for the A sub-lattice, thereby the net magnetic moment of the ferrite diminishes. Our calculated values of M_s shown in Table 1 are compared with the reported ones.[9,11] Das *et al.*[9] reported the value of $M_s \sim 60$ emu/gm for $x = 0.0$ and observed that the M_s decreases with increasing Sn concentration up to 5 wt.% in the Ni–Zn ferrites. Maskar *et al.*[11] obtained $M_s \sim 96$ emu/gm for $x = 0.0$ and noticed the lower M_s value for further substitution in Ni–Zn ferrites. We have found the value of $M_s \sim 72.2$ emu/gm, and a decreasing trend with increasing Sn content up to 40 wt.%, except for $x = 0.05$. A large discrepency of the saturation magnetization of pure Ni–Zn ferrite between this work and the reported results (Refs. [9] and [11]) is found as shown in Table 1. The large diversity of the reported M_s values might be due to the preparation techniques and conditions employed.

The Sn content dependence of the coercive field of NZSFO is depicted in Table 1. It shows that the H_c value increases with increasing Sn content which can be elucidated by the Brown's relation $H_c = 2K_1/\mu_0 M_s$, where K_1 is the anisotropy constant and μ_0 is the permeability of free space. As per the relation, the value of H_c is found to be increased with the decrease in the value of M_s. Furthermore, the Stoner–Wohlfarth single-domain theory proves that the H_c increases with the increase of the grain size.[29] The grain sizes of the prepared samples (NZFO and NZSFO) are also found to be increased with increasing Sn contents.[6] Therefore, it is expected to increase the value of H_c with the increase of x in the prepared samples. It could be noted that the values of H_c for the substituted samples are comparatively large. The large value of H_c for the substituted samples can be explained by the equation $H_c = \frac{\pi r}{M_s}(K_1/A)^{1/2}$, where A is the exchange stiffness constant, and r is the radius of the spherical pores.[30]

In general, the H_c varies directly with porosity and anisotropy and inversely with grain size.[30] Thus the H_c appears to be influenced by the magnetization and K_1, in addition to the microstructure.

The porosity of the NZSFO increases almost linearly with Sn concentration (approx. 27%–34%) while the porosity for the NZFO is of around 19%.[6] The grains size of the prepared samples (Table 1) is found to be increased from 10 μm to 34 μm with increasing Sn content ($0.05 \leq x \leq 0.3$) while the grain size of NZFO is only 7.8 μm. In addition, the increase in T_C suggests that the value of K_1 is also increased with increasing Sn content. It can be recalled that the value of M_s decreases with increasing Sn content. As a result, the value of H_c is much larger for the substituted samples (NZSFO).

The values of M_r and μ as a function of Sn concentration are also presented in Table 1. The mechanism for the variation of $\mu$and M_r is closely related to the M_s and H_c, respectively.

Figure 3 represents the real part of initial permeability (μ') and the imaginary part of the initial permeability (μ'') over the frequency range from 1 kHz to 100 MHz for the NZSFO for different Sn concentrations. The μ' and μ'' of the μ^* have been calculated using the following relations $\mu' = L_s/L_0$ and $\mu'' = \mu' \tan\delta$, where L_s is the self-inductance of the sample core and $L_0 = \frac{\mu_0 N^2 S}{\pi \bar{d}}$ can be derived geometrically. Here L_0 is the inductance of the winding coil without the sample core, N is the number of turns of the coil ($N = 5$), S is the cross-section area of the toroidal sample as given by $S = d \times h$, $d = (d_2 - d_1)/2$, d_1 is the inner diameter, d_2 is the outer diameter, h is the height, and $\bar{d}$ is the mean diameter of the toroidal sample ($\bar{d} = (d_2 + d_1)/2$). The real part of permeability μ' decreases with the frequency and the imaginary part of permeability μ'' exhibits a peak, which is related to the relaxation phenomenon. It is seen that the μ' remains almost

constant until the frequency is raised to a certain value and then drops to very low values at higher frequencies. The fairly constant μ' with a wide range frequency region is known as the zone of utility of the ferrite that demonstrates the compositional stability and quality of ferrites prepared by the conventional double sintering route. This characteristic is anticipated for various applications such as broadband pulse transformers and wide band read-write heads for video recording.[31] The value of μ'' gradually increases with the frequency and has a maximum at a certain frequency, beyond which μ' rapidly decreases. This feature is well known as the ferromagnetic resonance.[32] At higher doping concentration, the permeability is lower and the frequency of the onset of the ferromagnetic resonance is higher, which is in good agreement with Snoek's limit $f_r\mu' =$ constant,[33] where f_r is the resonance frequency for domain wall motion, above which μ' decreases.

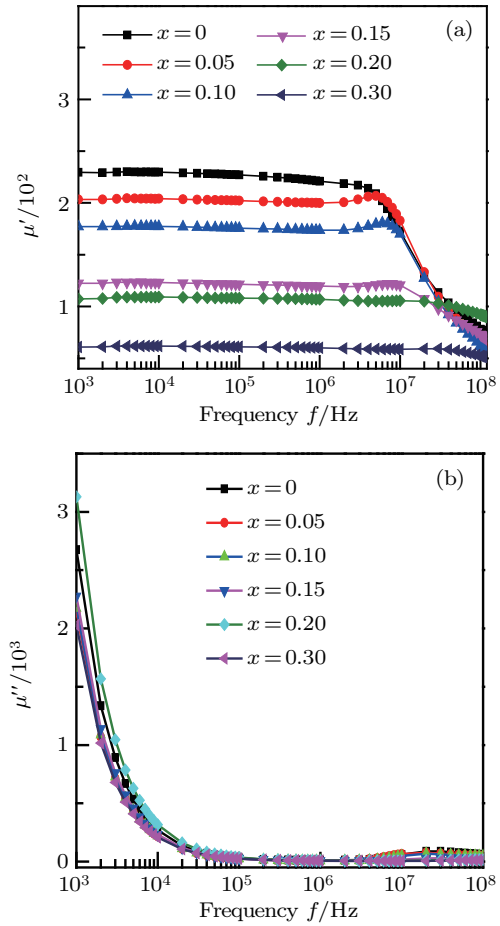


Fig. 3. (color online) The frequency dependence of permeability of the NZSFO with different Sn concentrations: (a) real part, (b) imaginary part.

Variation of μ' with Sn concentration at 1 MHz frequency is shown in Fig. 4(a). The decrease in the initial permeability of the Ni–Zn ferrites can be explained using the following equation $\mu' = M_s^2 D/\sqrt{K_1}$, where D is the average grain size. As μ' is proportional to the square of the saturation magnetization and the saturation magnetization decreases with the increase in Sn concentration, the value of μ' is expected to be decreased. Tetravalent Sn^{4+} ions have a strong octahedral-site preference, and the saturation magnetization decreases with increasing Sn^{4+} substitution due to the weaker A–O–B superexchange interaction, which results in the decrease of μ'.[34] Figure 4(b) shows the relative quality factor of NZSFO. The peak corresponding to maxima in Q-factor shifts to a higher frequency as the Sn content increases. The Q-factor has the maximum value of 5.2×10^3 at $f = 20$ MHz for the $x = 0.05$ sample. The Q-value depends on the ferrite microstructure, e.g. pore, grain size, etc.

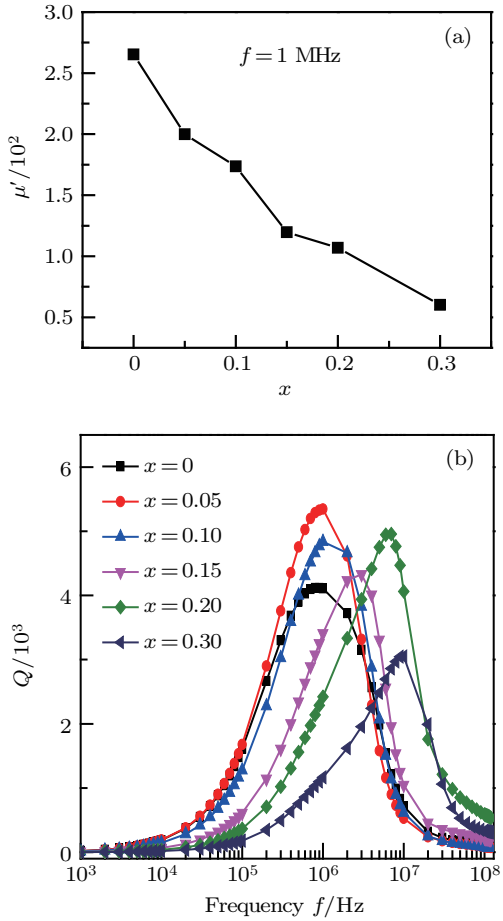


Fig. 4. (color online) Variation of (a) μ' with Sn concentration at 1 MHz, (b) variation of Q-factor with frequency for NZSFO ferrites with different Sn concentrations.

Curie temperature T_C is the transition temperature above which the ferrite material loses its magnetic properties. The temperature dependence of initial permeability μ' of the toroid shaped sample of NZSFO at constant frequency 1 MHz of an AC signal is shown in Fig. 5(a). The initial permeability increases rapidly with increasing temperature and then drops off sharply near the transition temperature known as T_C showing the Hopkinson effect.[35] A significant peak is obtained near T_C where the value of K_1 becomes almost negligible. At T_C, complete spin disorder takes place, i.e., a ferromagnetic material converts to a paramagnetic material. The T_C gradually

increases with increasing Sn concentration excluding $x = 0.05$ where it is decreased moderately as shown in Fig. 5(b).

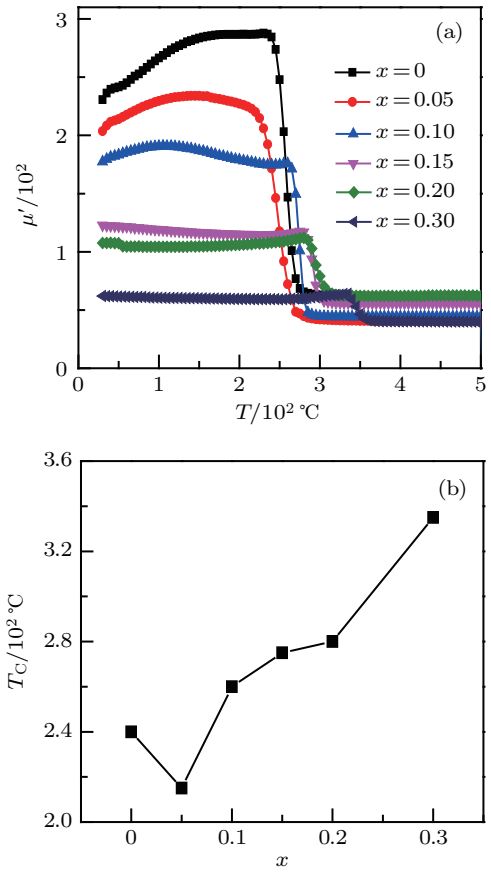


Fig. 5. (color online) (a) Temperature dependent initial permeability (μ') for different Sn concentrations, (b) variation of the Curie temperature T_C as a function of Sn concentration in the NZSFO ferrites.

It can be explained as follows. Initially, the dopant cations are assumed to occupy tetrahedral (A) sites and they enter into B sites due to further increase of dopant cations thereby pushing some Fe^{3+} ions to A-sites, resulting in the magnetic ion density decrease in the B sub-lattice.[9] The increase of the magnetic ions in the A sites increases the A–B interaction, consequently increasing the T_C (Fig. 5(b)). However, the mechanism of the T_C decreasing in a particular point has not been understood yet.

Finally, from Table 1, it is evident that the sample with $x = 0.05$ shows unusual results. The saturation magnetization of the substituted samples is less than that of the parent one except for $x = 0.05$. Moreover, the T_C values are fairly linear with Sn content except for $x = 0.05$. This unusual behavior might be explained by assuming that initially at lower Sn concentrations ($0 \leq x \leq 0.1$), the Sn ions occupy tetrahedral (A) sites while these ions reside in octahedral (B) sites at higher Sn concentrations.[9] This can be confirmed by other investigations such as neutron diffraction, but unfortunately we are unable to perform such investigation and left this issue to other researchers for further study.

4. Conclusion

Sn-substituted polycrystalline ferrites, NZSFO ($x = 0.0$, 0.05, 0.1, 0.15, 0.2, and 0.3) sintered at 1300 °C, have been successfully synthesized using standard ceramic technique. The single phase spinel structure of the samples has been confirmed by the XRD patterns. The grain size increases from 7.8 μm to 34.8 μm with increasing Sn content. The saturation magnetization is found to be decreased with increasing Sn concentration while the coercivity is increased. The initial permeability is fairly constant up to 10 MHz, i.e., a wide range of operating frequency or stability region has been achieved for the samples. The Curie temperature rises gradually with increasing Sn content, except $x = 0.05$, which is fruitfully explained by the variation of A–B interaction strength due to dopant cations entering into different sites. A reasonably low H_c for $x = 0.0$ implies that this material is a promising candidate for transformer core and inductor applications.

Acknowledgements

The authors are grateful to the Directorate of Research and Extension, Chittagong University of Engineering and Technology (CUET), Chittagong-4349, Bangladesh under grant number CUET/DRE/201415/PHY/002 for arranging the financial support for this work. We are also thankful for the laboratory support of the Materials Science Division, Atomic Energy Commission, Dhaka 1000, Bangladesh.

References

[1] Chen Q, Du P, Huang W, Jin L, Weng W and Han G 2007 *Appl. Phys. Lett.* **90** 132907
[2] Sugimoto M 1999 *Ceram. J. Am. Soc.* **82** 269
[3] Smit J and Wijn H P G 1959 *Ferrites* 136
[4] Eerenstein W, Mathur N D and Scott J F 2006 *Nature* **442** 759
[5] Ali M A, Khan M N I, Chowdhury F U Z, Akhter S and Uddin M M 2015 *J. Sci. Res.* **7** 65
[6] Ali M A, Uddin M M, Khan M N I, Chowdhury F U Z and Haque S M 2017 *J. Magn. Magn. Mater.* **424** 148
[7] Khan D C, Misra M and Das A R 1982 *J. Appl. Phys.* **53** 2722
[8] Khan D C and Misra M 1985 *Bull. Mater. Sci.* **7** 253
[9] Das A R, Ananthan V S and Khan D C 1985 *J. Appl. Phys.* **57** 4189
[10] Khan D C, Srivastava R C and Das A R 1992 *J. Phys.: Condens. Matter* **4** 1379
[11] Maskar P K, Kakatkar S V, Patil R S, Jadhav V A, Chaudhari N D, Sankpal A M and Sawant S R 1995 *Mater. Chem. Phys.* **41** 154.
[12] Mundada O G, Jadhav K M and Bichile G K 1997 *J. Mater. Sci. Lett.* **16** 432
[13] Prasad M S R, Prasad B B V S V, Rajesh B, Rao K H and Ramesh K V 2011 *J. Magn. Magn. Mater.* **323** 2115
[14] Kaiser M 2012 *Physica B* **407** 606
[15] Kaur B, Arora M, Shankar A, Srivastava A K and Pant R P 2012 *Adv. Mat. Lett.* **3** 399
[16] Hashim M, Alimuddin, Kumar S, Ali S, Koo B H, Chung H and Kumar R 2012 *J. Alloy. Compd.* **511** 107
[17] Mandal A, Ghosh D, Malas A, Pal P and Das C K 2013 *J. Engg. Art. ID* 391083
[18] Yoo B S, Chae Y G, Kwon Y M, Kim D H, Lee B W and Liu C 2013 *J. Magn.* **18** 230
[19] JanČárik V, UŠák E, Šoka M and UŠáková M 2014 *Acta Physica Pol. A* **126** 90

[20] Kwon Y M, Lee M Y, Mustaqima M Liu C and Lee B W 2014 *J. Magn.* **19** 64

[21] Ateia E E, Ahmed M A, Salah L M and El-Gamal A A 2014 *Physica B* **445** 60

[22] Köseoğlu Y 2015 *Ceram. Int.* **41** 6417

[23] Kumar R, Kumar H, Kumar M, Singh R R and Barman P B 2015 *J. Super. Nov. Magn.* **28** 3557

[24] Hedayati K 2015 *J. Nanostructure* **5** 13

[25] Kumar R, Kumar H, Singh R R and Barman P B 2015 *AIP Conf. Proc.* **1675** 030003

[26] Wang S F, Hsu Y F, Chou K M and Tsai J T 2015 *J. Magn. Magn. Mater.* **374** 402

[27] Ashtar M, Maqsood A and Anis-ur-Rehman M 2016 *J. Nanomater. Mol. Nanotechnol.* **5** 3

[28] Ishaque M, Khan M A, Ali I, Athair M, Khan H M, Iqbal M A, Islam M U and Warsi M F 2016 *Mater. Sci. Semi. Proc.* 41508

[29] Stoner E C and Wohlfarth E P 1991 *IEEE Trans. Magn.* **27** 3475

[30] Baha P D 1965 *J. Am. Ceram. Soc.* **48** 305

[31] Zabotto F L, Gualdi A J, Eiras J A, de Oliveira A J A and Garcia D 2012 *Mater. Res.* **15** 428

[32] Brockman F G, Dowling P H and Steneck W G 1950 *Phys. Rev.* **77** 85

[33] Snoek J L 1948 *Physica* **14** 207

[34] Sun K 2008 *J. Magn. Magn. Mater.* **320** 1180

[35] Overshott K J 1981 *IEEE Trans. Magn.* **17** 2698